CHEMICALLY MODIFIED ELECTRODES. RADIOFREQUENCY PLASMA POLYMERIZATION OF VINYLFERROCENE ON GLASSY CARBON AND PLATINUM ELECTRODES

R. J. Nowak, F. A. Schultz, M. Umana, R. Lam and Royce W. Murray
Kenan Laboratories of Chemistry
University of North Carolina
Chapel Hill, North Carolina 27514

ABSTRACT

Vinylferrocene can be polymerized in a radiofrequency Ar plasma to deposit in thin, adherent films on glassy carbon and Pt electrodes. In acetonitrile solvent containing tetraethylammonium perchlorate or tetrafluoroborate electrolyte, these films exhibit electrochemical reactivity qualitatively expectable for polyvinylferrocene films although analytical information on film composition shows some plasma damage and some oxygen incorporation has taken place. The relationship of observed electrochemistry to plasma reaction time and geometry is described. Quantities of electroactive ferrocene in the prepared films range from 0.5 - 300 x 10^{-10} mole/cm.^{2}. The thinner films exhibit non-limiting transport of electrochemical charge, while a thick film gives a diffusion-controlled response.

BRIEF

Vinylferrocene polymer films deposited from Ar radiofrequency plasmas on C or Pt electrodes exhibit multimolecular layer electrochemical responses in acetonitrile solvent.

CHEMICALLY MODIFIED ELECTRODES. RADIOFREQUENCY PLASMA POLYMERIZATION OF VINYLFERROCENE ON GLASSY CARBON AND PLATINUM ELECTRODES

R. J. Nowak, F. A. Schultz, M. Umaña, R. Lam and Royce W. Murray
Kenan Laboratories of Chemistry
University of North Carolina
Chapel Hill, North Carolina 27514

The preparation and properties of electrodes coated with thin films of polymeric materials has been the object of a number of recent investigations (1-11). By virtue of adsorptive interactions with the electrode and/or low solubility in the contacting solvent (1-6), or chemical bonding to the electrode (7-9), the polymer coatings can be stable to contact with solvent/electrolyte media and to use in electrochemical experiments. Electroactive materials dissolved in the solvent undergo electrochemical reactions at polymer coated electrodes (1,2,4) although inhibition of electrochemistry is also observed (1). Generalities of mass transport through channels or pinholes (2) and electronic charge transport (10) are unsettled, significant questions.

Electroactive moieties which are fixed constituents of the polymer coating itself (e.g., redox polymers) also undergo electrochemical reaction with the electrode (1-9). Redox polymer films on electrodes have been prepared by dip coating (1), organosilane reactions (7-9), slurry spreading (5), electrochemical polymerization (6), electrochemical precipitation (2), and radiofrequency plasma polymerization (9a).

The mechanism(s) which permit electron transfer between electrode/polymer interface and fixed electroactive sites, over distances of hundreds of Angstroms (4,5,11), is an interesting aspect of redox polymers. It seems clear that the long range transport of electrochemical charge through redox polymer films will be affected as much by properties of the polymer lattice (e.g., the degree of swelling by solvent, penetration by electrolyte ions, internal lattice mobility, electronic conductivity, etc.) as by those of the electroactive site itself. An ability to vary polymer lattice properties, and film thickness, should therefore be important in understanding, and exploiting, long range charge transport in polymers.

The introduction of various monomers into radiofrequency plasma discharges is known (12) to initiate polymerization reactions and deposition of polymer films on walls of the plasma chamber and on objects placed therein. The polymerization reactions in electrodeless discharge experiments are thought to occur in the plasma gas with surface deposition of the plasma polymer film proceeding at a rate which is a function of plasma chamber geometry, monomer pressure and flow rate, radiofrequency power, and substrate temperature (13-15). The energetic plasma environment typically leads to some molecular fragmentation and cross-linking in the polymer which tends to have a complex composition (12). Composition may vary with deposition rate. Molecular weight distributions are most often unknown and are probably wide in general. Plasma deposited films can display (ESR) unpaired electron sites which persist for long periods of time and films are known to undergo some oxygen up-take on exposure to air (12).

Although coating of electrodes by electrochemically passive, plasma discharge films has been reported (10), deliberate incorporation of electron transfer moieties into films plasma deposited on electrodes had not been described prior to our preliminary experiments with vinylferrocene monomer in

in a radiofrequency plasma (9a). Those experiments produced multimolecular layer films in which charge migrated rapidly between ferrocene sites and the Pt or glassy carbon substrate, and which, in keeping with the general reputation of plasma deposited films (12), were very durable. Properties of the films varied with details of the plasma experiment, and so we initiated a study of several experimental variables, results of which are reported here. In particular, we have examined the consequences of reactor geometry, plasma deposition times, and electrode substrate (Pt versus glassy carbon). Some results on chemical composition of the film are also presented.

EXPERIMENTAL

Plasma Experiment. A 10-15 watt inductively coupled radiofrequency plasma was generated in a Harrick Scientific (Ossining, N.Y.) plasma unit. The system was pumped by an L_{N_2} trapped two-stage mechanical pump, monitoring pressure with a thermocouple gauge.

Our reactor design differs from most by placing solid monomer (vinylferrocene) in the plasma discharge region along with the electrode to be coated, rather than flowing monomer into the plasma discharge. This provides a high monomer pressure in the immediate vicinity of the sample as well as the advantage of an extremely simple experimental arrangement. Placement of the monomer reservoir with respect to electrode surface (e.g., experiment geometry) is important. Figure 1 illustrates the different geometries used in this study. Geometry A was used initially, successfully, but not very reproducibly, and results reported are for Geometries B and C.

In a typical experiment, glassy carbon and vinylferrocene monomer were placed in the plasma chamber which was alternatively evacuated and filled with argon several times (RF power off), the final time to 200 mtorr, and

the RF power then set at the lowest power setting (ca. 10 watts) producing a plasma discharge. After the deposition period, the RF power was turned off, the chamber evacuated, air bled in slowly, and the electrodes removed and stored in air or under solvents as indicated. Exposure of electrodes to vinylferrocene vapor in this manner with RF power off yields no electrochemical or other evidence of immobilized ferrocene.

Electrochemical Experiment. Cyclic voltammetry was performed with PARC Model 173 or 174 potentiostats using a triangle wave generator of published design (16). The electrochemical cell was conventional with a Luggin probe, Pt auxiliary electrode and either plasma coated glassy carbon (Atomergic Chemetals Corp.) or Pt disk working electrodes. Potentials are referenced to a NaCl-saturated calomel electrode (SSCE). Glassy carbon and Pt electrodes were polished to a mirror finish (one μm diamond polishing compound, Metadi, Buehler) and degreased with solvents before plasma coating. Glassy carbon electrodes were mounted on glass tubes for electrochemistry using heat shrink Teflon tubing, leaving only the polished cylinder end exposed to the solution. A thin film of silicone grease was present on the carbon cylinder sides to prevent solution intrusion. Pt electrodes (6.4 mm diameter disks), with a Pt wire spot-welded on the reverse face, were lowered in the cell to just make contact with the solution. No device to mask the sides of the electrode disk was thus necessary.

Spectra. X-ray (Mg anode) photoelectron spectra were obtained with a DuPont 650B electron spectrometer (17) interfaced to a microcomputer system. Scanning electron micrographs and X-ray fluorescence data were obtained with an ETEC Autoscan scanning electron microscope equipped with an energy dispersive X-ray spectrometer (Kevex 500). Magnifications are corrected for working distance.

Elemental Analysis. Analyses were performed by Galbraith Laboratories on plasma polymerized ferrocene and vinylferrocene, deposited for ten minutes onto a glass microscope slide (Geometry B). No special precautions were taken to protect the harvested sample from the atmosphere after removal from the chamber. Analyses: plasma polymerized ferrocene, % Found: 48.43 C, 5.18 H, 25.88 Fe; plasma polymerized vinylferrocene, % Found: 56.28 C, 5.47 H, 23.96 Fe.

Chemicals. Vinylferrocene (Pfaltz and Bauer), and tetraethylammonium tetrafluoroborate (Southwestern Analytical Chemicals, Inc.), were used as received. Acetonitrile (Spectrograde, MCB) and methylene chloride (Fisher) were stored over activated molecular sieves (Davison, grade 513, 4A). Tetraethylammonium perchlorate (Eastman) was recrystallized thrice from water.

RESULTS AND DISCUSSION

The result of a very short (15 second) plasma deposition period on a glassy carbon electrode is shown in Figure 2. The observed cyclic voltammetric wave occurs at a potential consonant with a ferrocene⇌ferricenium reaction in acetonitrile and exhibits properties of a surface-immobilized species (18), e.g., symmetry, potential sweep rate (v) independent difference in cathodic and anodic peak potentials (ΔE_p), ΔE_p less than 59 mv., and peak current (i_p) proportional to v (Figure inset). This and cyclic voltammograms described below persist for long periods of potential cycling and exposure to the solvent.

The short deposition time surface coverage by electroactive ferrocene in Figure 2 is quite small, $\Gamma = 0.5 \times 10^{-10}$ moles/cm.$^{-2}$, corresponding to an average 22 Å ferrocene spacing (assuming all immobilized ferrocenes undergo

electron transfer and zero surface roughness). The average surface coverage by polymerized vinylferrocene in this example is less than monomolecular in ferrocene sites. Coverages of nearly 1000x this value can be obtained by changing geometry, substrate, deposition time: the dynamic range of preparable polymer film thickness is very large.

Composition of Plasma Polymerized Vinylferrocene Films. Although vinylferrocene has been reported to be an efficiently polymerizable monomer (19), we have found no previous analytical characterization of the polymer product. The survival of the ferrocene $\rightleftharpoons$ ferricenium moiety in plasma polymerized vinylferrocene is unambiguously established by the electrochemical behavior of Figure 2. The formal potential, E°', of the film's ferrocene wave, in $Et_4N^+ClO_4^-/CH_3CN$ solvent, varies among different samples from 0.38 to 0.42 volt vs. SSCE. Formal potentials for dissolved ferrocenes with α-carbonyl functions (20), such as ferrocene carboxylic acid, +0.63 volt vs. SSCE do not agree with the film's observed formal potential and appear to not be important ingredients of the film. The E°' for dissolved vinylferrocene monomer is similar, +0.40 volt vs. SSCE, but films prepared (21) from conventionally prepared, authentic polyvinylferrocene also show E°' = +0.37 to +0.41 volt vs. SSCE. On the basis of formal potential, in acetonitrile the ferrocene sites in the plasma polymer film seem substitutionally similar to those of immobilized polyvinylferrocene, e.g., $\text{-}(CH_2\dot{C}H)\text{-}C_5H_4FeC_5H_5$.

The plasma polymer film is clearly however not composed entirely of the simple ferrocene monomer. The elemental analysis of harvested samples of plasma-deposited polymer gives 15% of unaccounted mass; if this is assumed to be oxygen, the empirical formula is $FeC_{11}H_{12.6}O_2$. X-ray photoelectron spectroscopy described elsewhere (22) reveals a Fe $2p_{3/2}$ band at 708.5 e.v. (ferrocene binding energy) and a broad band at ca. 711 e.v. binding energy which we believe is in part ferricenium and in part a non-electroactive Fe(III)

plasma decomposition product firmly affixed to the polymer lattice. The relative intensities of the 711 e.v. and 708.5 e.v. bands are related to the extent of exposure of the film's surface to argon ion bombardment during film deposition. In experiments described in this paper, the 711 e.v. band was quite prominent in the polymerized vinylferrocene films. Much more rapid deposition conditions (21) yield very little plasma damage, e.g., a dominant 708.5 e.v. peak and a small 711 e.v. peak. The latter material also shows oxygen uptake by its empirical formula of $FeC_{10}H_{11}O_{1.7}$, so the presence of the 711 e.v. peak does not correlate simply with the existence of oxygenated sites in the film. We do not know the chemical nature of the oxygenated sites but by $E^{\circ\prime}$ as noted above they are not attached directly to the ferrocene nucleus.

A direct measurement of the thickness of the plasma polymerized vinylferrocene film was attempted by scanning electron microscopy. A specimen with a large quantity of electroactive ferrocene, 3×10^{-8} mole/cm.^{2}, was used for this experiment. Gross morphology of the film, deposited for a 10-minute reaction time from Geometry B on glassy carbon (vide infra), is shown in Figure 3, Panel A. As compared to uncoated, freshly polished (1 μm diamond paste) glassy carbon, which shows faint polishing grooves (Panel A inset), the plasma coated electrode surface is randomly dimpled, without grooves. (The ca. 2 μm pits are typical pores of our glassy carbon and are scattered across its surface). The coated electrode shows no evidence for clumps of particulate matter. The film thickness was estimated by gently drawing a razor blade across the surface of the electrode of Panel A. In the STM (Panel B), the top portion of the photograph is undisturbed film; the bottom is the scratch track where the film was removed.

This was confirmed by the distribution of iron over this same field of view using X-ray fluorescence; the top portion showed an even distribution of iron and the bottom none. Estimation of the "step" height yields a film thickness of about 1000 Å which with the 3×10^{-8} mole/cm.^{2} coverage yields 3×10^{-3} mole/cm.^{3} for the concentration of ferrocene sites in the film. This concentration must be considered a lower limit since mechanical bulging of the cut film's lip plus some removal of carbon may occur in Figure 3B.

For comparison, if the film were assumed to be pure polyvinylferrocene with a density of 1.4 g/cm^3, the concentration of ferrocene sites would be 6.6×10^{-3} mole/cm.^{3}. The 3×10^{-8} mole/cm.^{2} coverage would predict a film dimension approximately half as big as the thickness measurement, 450 Å. The factor of two agreement is considered satisfactory at the present time given uncertainty of the SEM measurement and the presence of plasma damaged (and non-electroactive) iron(III) sites in this film. It is also presently conceivable that some ferrocene sites spatially remote in the film from the electrode surface may be silent in the film's electrochemistry.

Deposition and Reprecipitation. In a further characterization, an experiment like that by Merz and Bard (2) (on authentic polyvinylferrocene) was performed using vinylferrocene plasma polymerized as a film on a glass slide (Geometry B, 5 minute deposition). Most (not all) of this film slowly dissolved upon contact with CH_2Cl_2 containing 0.1 M Bu_4NClO_4. Cyclic voltammetry of this CH_2Cl_2 polymer solution at Pt revealed a solution wave of normal appearance (i_p proportional to $\sqrt{v}$) at +0.40 ± 0.01 volt vs. SSCE. The Pt electrode was then potentiostated at +0.8 volt for 10 minutes, disconnected, removed from the CH_2Cl_2, rinsed, and examined by cyclic voltammetry in 0.1 M Et_4NClO_4/acetonitrile. Similar to the result (2) of

Merz and Bard, a surface wave was observed for immobilized ferrocene (Figure 4) transferred on the electrode surface to the acetonitrile medium. $E^{\circ\prime}$ was 0.39 volt vs. SSCE (which is within the range of values observed for various intact plasma polymerized vinylferrocene films) and ΔE_p = 40 mv. at v = 0.02 volt/sec.

The Merz-Bard (2) dissolution-reprecipitation experiment, in which plasma polymerized vinylferrocene behaves like polyvinylferrocene, demonstrates similar solubility properties for the two materials. If the experiment is performed with a CH_2Cl_2 solution of vinylferrocene monomer, no surface cyclic voltammetric waves are observed on the transferred Pt electrode in acetonitrile. This shows that the plasma polymerized material contains ferrocene sites as integral constituents of the polymer as opposed to vinylferrocene monomer or very short polyvinylferrocene chains physically trapped in an organic polymer matrix.

The anodic and cathodic waves in the cyclic voltammogram of Figure 4 exhibit a slight tailing reminiscent of the cyclic voltammetry of a diffusing solution reactant, although the polymer film is immobilized on the electrode surface. Measured by a baseline extrapolation as shown in the figure, the quantity of charge for the anodic wave varied from 3.8 to 6.1 x 10^{-9} mole/cm.^{2} over v = 0.5 to 0.05 volt/sec. The tailing makes accurate estimation of baseline charge difficult. A smaller proportion of the ferrocene reacts in the fast sweep experiments. This peak shape and sweep rate dependency is also a property of some plasma polymerized films as discussed below.

Electrochemistry of Solution Reactants at Polymer Coated Electrodes. Glassy carbon electrodes exposed to vinylferrocene plasma polymerization for various deposition times were employed in acetonitrile solvent as electrodes for tetracyanoquinodimethane (TCNQ) reduction. TCNQ normally undergoes two single

electron reductions with $E_1^{o'}$ = +0.195 and $E_2^{o'}$ = -0.350 volt vs. SSCE in 0.1 M Et_4NClO_4/acetonitrile. Figure 5A illustrates TCNQ cyclic voltammetry at glassy carbon freshly coated with a modest coverage of polymerized vinylferrocene (Γ = 1.2 x 10^{-10} mole/cm.^{2}, independent of v = 0.05 to 0.5 volt/sec.) and after extensive cycling (3000 scans in absence of TCNQ) through the ferrocene wave such that electroactive ferrocene coverage has decayed to $\Gamma \approx 0.5 \times 10^{-10}$ mole/cm.^{2} (Figure 5B). On the fresh electrode, ΔE_p was 10 mv. for the ferrocene wave and 65 and 85 mv. for the TCNQ waves, which were not affected at all by the polymer. On the extensively cycled electrode, on the other hand, both TCNQ waves are sharply attenuated and quite irreversible.

On other, more heavily, freshly coated electrodes ($\Gamma \sim 10^{-9}$ mole/cm.^{2}), TCNQ electrochemistry likewise becomes inhibited. Similar correlation of high coverage with inhibition properties toward TCNQ was observed for polymer coatings on Pt electrodes.

These experiments suggest that TCNQ access to the electrode is restricted by these ferrocene polymer films. At low film coverages, the absence of inhibition (Figure 5A) could be interpreted as free TCNQ dissolution into the thin film. The aging effect suggests, on the other hand, that this penetration into the fresh electrode probably involves channels and pinholes, which become covered by polymer chain reconstruction during extended ferrocene $\rightleftharpoons$ ferricenium cycling, or by heavy initial plasma deposition. Possibilities for annealing of channels and pinholes in ultrathin films have not been noted in previous studies (1,2,10).

Plasma Reaction Geometry. Numerous plasma polymerization studies have identified the importance of reactor geometry on polymer deposition rate. In a given tubular reactor geometry, the deposition rate can vary with axial

position as shown in a study of acetylene and ethylene (23).

The effect of position of the electrode sample in Geometry C (Figure 1) was studied by placing three Pt electrodes at varying distances, 2, 5, and 8 cm, from the monomer source, coating all simultaneously. The axial distance effect was substantial. Using a deposition time of one minute, Figure 6A, 6B shows that while formal potential $E^{o'}$ of the ferrocene wave remains constant, the quantity of deposited electroactive ferrocene polymer decreases between the 2 and 8 cm electrode positions by a factor of about six. (The third sample had an intermediate coverage). The higher coverage sample (Figure 6A) additionally displays an altered cyclic voltammetric shape (solution reactant-like), a larger ΔE_p (80 mv.), and a dependence of apparent coverage (charge above extrapolated baseline) on potential scan rate, $\underline{v}$.

Thus, reactor geometry affects film deposition rate, as expected, and its control is important for achieving reproducible film thicknesses by plasma polymerization. Whether other factors (e.g., chain length, cross-linking, O_2 incorporation) become interrelated with reactor geometry and deposition rate is a question not yet satisfactorily answered.

Substrate Electrode Material. Our initial plasma deposition experiments were carried out with glassy carbon electrodes with the expectation (drawing analogy from work with argon plasma which produced oxide free carbon surfaces) (24) that some chemical binding of the polymerized vinylferrocene to the electrode surface would occur. Evidence exists that this indeed occurs (21) but only for the first layer or two of polymer chains. Binding of the polymer to the electrode is not essential, however, since quite stable electrochemical responses also occur in appropriate solvents for plasma coated Pt electrodes (where binding is thought not to occur).

Plasma deposition on glassy carbon and Pt may also differ because of the conductive nature of these materials and the different masses of the elec-

trodes. Some inductive heating probably occurs in the plasma. Additionally, the plasma discharge is to some extent quenched in the immediate vicinity of the electrodes (this has been visually observed on a few occasions). This quenching effect may vary with electrode material, its mass, and geometrical placement in the plasma, producing differences in deposition rate and possibly other polymer properties.

To examine the effect of substrate electrode, both glassy carbon and Pt were tested in both Geometries B and C (Figure 1). In Geometry C, plasma deposition for equal periods on glassy carbon and Pt electrodes produces lower (4-10x) coverages on glassy carbon.

In Geometry B, some voltammetric shape differences were observed. Figure 6C, 6D illustrates steady state cyclic voltammograms for three minute deposition times on platinum and glassy carbon electrodes. After accounting for the different electrode areas ($A_{Pt}/A_C = 4.5$), the peak current densities and the coverages are nearly the same; $\Gamma = 6.8$ and 4.7×10^{-10} mole/cm.^{2} for Pt and glassy carbon, respectively. The $E^{\circ\prime}$ differ by about 45 mv. Deposition on Pt in Geometry B (Figure 6C) produces a symmetrically shaped surface wave, like deposition on Pt at similar coverage in Geometry C (Figure 6B). On glassy carbon, however, (Figure 6D), the anodic current peak is substantially narrower than the cathodic peak. This dissymmetry tends to go away (the anodic peak broadens) after the electrode is cycled a number of times, i.e., a conditioning effect.

Deposition Time. The mass of deposited polymer in electrodeless RF discharges under continuous flow conditions has been reported (25) to increase linearly with time. The relationship between film thickness and deposition time in the present experiment was investigated for Pt electrodes (in Geometry C) and glassy carbon electrodes (in Geometry B) by examination

of the cyclic voltammetry. Figure 7 shows deposition time dependence of polymer coverage as measured by the cyclic voltammetric wave for electroactive ferrocene. Each point, with standard deviation, is the average of anodic and cathodic peak charges (coverages) obtained at several sweep rates for a single electrode. The large standard deviation for high coverage platinum electrodes reflects dependency of the apparent coverage on sweep rate like that noted for Figure 6A.

A correlation obviously exists between deposition time and the quantity of electroactive ferrocene in the plasma polymer. Whether the relationship is accurately linear or not is obscured by the afore-mentioned sweep rate effect for Pt in Geometry C and by scatter in the coverage values. In general, platinum electrodes (Geometry C) yield larger coverage than glassy carbon electrodes (Geometry B).

XPES spectra measured for the Pt electrode deposition time series, after each specimen had been inspected by cyclic voltammetry, were in qualitative accord with the trend in electrochemical coverage. With increasing deposition time, the Pt 4f bands become increasingly attenuated, and the Fe $2p_{3/2}$ band grows. Ratios of the intensities of these two bands are noted for several points on Figure 7.

Charge Transport Effects. For both carbon and Pt electrodes, short deposition time and low coverage yield symmetrically shaped voltammograms like those in Figures 2, 6B and 6C. Such symmetry is expected for reversible (fast charge transfer) surface waves (18) where the total population of electroactive surface sites remains at or near thermodynamic equilibrium at each applied potential.

Significant alterations in symmetry of the cyclic voltammetric waves are observed as coverage increases in Figure 7. On Pt, deposition of thicker

vinylferrocene polymer films (longer deposition time, or proximity in Geometry C, e.g., Figure 6A) leads to tailing of the anodic and cathodic branches of the cyclic voltammogram. This voltammetric shape is further illustrated in Figure 8, where data taken at several potential sweep rates are given. It plausibly reflects kinetic limitations on the rate at which ferrocene sites in the polymer become oxidized and re-reduced. Since both equilibrium (low coverage) and kinetically controlled behaviors occur for the same charge transfer center (ferrocene), the kinetic phenomena must be ascribed to the polymer environment in which the ferrocene sites are imbedded, not to intrinsic properties of ferrocene itself. This point has general importance for understanding multilayer modified electrodes.

Our analysis of the high coverage voltammograms of Figure 8 is based on its shape which is reminiscent of cyclic voltammograms of solution reactants. Figure 8 shows that the anodic (and cathodic) peak currents, i_p, are proportional to the square root of potential sweep rate, $\sqrt{v}$, not directly proportional to v as normally expected for surface reactants. Peak current separation ΔE_p is throughout > 60 mv. The charge under the voltammetric wave (measured as indicated) varies substantially with v, even if baseline current is arbitrarily included in the charge. The sweep rate dependency of charge is associated with the appearance of the tailing wave shape, being absent at lower coverages where waves are symmetrical (Figure 2, 6B-D). Obviously, a good deal of electroactive ferrocene remains unoxidized as the potential is swept through the peak, more so at fast sweep rates.

The properties of the waves in Figure 8 are those expected for an electrochemical reaction controlled by diffusion. In effect the transport of electrochemical charge between Pt and ferrocene and ferricenium sites is a diffusional process. Furthermore, the proportionality of i_p and $v^{1/2}$ in

cyclic voltammetry, in the Randles-Sevcik equation (26), is based in theory on a semi-infinite volume of diffusing reactant in contact with the electrode, such that the depletion layer of the diffusion profile never reaches the cell wall. The "cell" dimension of the Figure 8 experiment is the thickness of the plasma polymerized vinylferrocene film itself, which is quite small. For the $\underline{i_p - v^{1/2}}$ result of Figure 8 to be obtained, therefore, the rate of diffusion of electrochemical charge through the polymer must be very slow in comparison to diffusion rates familiar in electrolyte solutions.

If the Randles-Sevcik equation is applied to the $\underline{i_p - v^{1/2}}$ slope in Figure 8, a value of $CD^{1/2} = 9.4 \times 10^{-9}$ mole/cm.-sec. results, where $\underline{C}$ is the concentration of ferrocene sites in the polymer. The results for $\underline{C}$ above, $3 - 6.6 \times 10^{-3}$ mole/cm.^{3}, do not strictly apply to the situation of polymer film electrochemistry, since we believe the plasma polymerized vinylferrocene film is moderately swollen by the acetonitrile solvent. No good quantitative data however are available for the degree of swelling. If we take the smaller 3×10^{-3} mole/cm.^{3} concentration for $\underline{C}$ a value of $\underline{D} \sim 9.8 \times 10^{-12}$ cm.^{2}/sec. is obtained for the plasma film of Figure 8. This very slow transport rate plus adherence to semi-infinite diffusion theory leads to the prediction that the film thickness exceeds $(\underline{Dt})^{1/2}$ where $\underline{t}$ is time of the electrochemical experiment. Taking t = 2 seconds, thickness > 450 Å, in accord with the estimates above.

The process of electrochemical charge transport surely involves migration between fixed ferrocene and ferricenium sites in the film, but electron hopping accompanying this will be a movement of counterions and co-ions of the ferricenium sites, plus associated solvent molecules. The present analysis does not permit a specific molecular correlation of $\underline{D}$ with any one of these or other

conceivable motions. This important question has been further pursued using plasma deposited vinylferrocene polymer films less plasma damaged (smaller 711 e.v. XPES peak) in which the transport of electrochemical charge occurs at much faster rates. By using lowered temperature we have been able to vary electrode response from Nernstian to finite diffusional to semi-infinite diffusional and to quantitatively account for these responses, confirming the interpretation above. These data and consideration of the molecular nature of the diffusion process will be presented elsewhere.

CONCLUSIONS

Although the analytical information on plasma polymerized vinylferrocene indicates an overall compositional difference from the ideal polyvinylferrocene plasma product, the electrochemical properties of films of this substance are accountable by oxidation-reduction reactions of ferrocene-ferricenium sites attached to polymer chains in the film. These electrochemical properties can be obtained reproducibly in successive plasma experiments provided the importances of plasma reactor geometry, plasma deposition time, and electrode substrate material are recognized and controlled. The plasma polymerized vinylferrocene films can be considered a useful redox polymer system for study of transport of electrochemical charge and of solution species through the polymer. Considering the potential importance of these transport events in electrocatalytic, photoelectrocatalytic, and electrochromic applications of redox polymer-coated electrodes, the slow electrochemical charge transport (Figure 8) and solution reactant penetration (Figure 5) experiments reported here have some significance.

We observed two kinetic situations in these experiments. Some electrodes, notably at low coverage, exhibit symmetric waves with i_p proportional to v, which is diagnostic of fast electrochemical charge transport. The entire film's array of ferrocene-ferricenium sites stay in Nernstian equilibrium wih the Pt or carbon electrode potential on the cyclic voltammetric time scale. Other electrodes, notably at high coverages, display diffusionally limited electrochemical charge transport. These two situations can be considered kinetic extremes of a common mechanism for migration of charge through the polymer. Kaufman and Engler (5) have proposed a site-site collisional electron exchange mechanism for a different redox polymer, but offered no quantitative evidence for the expected diffusional character. In light of our quantitatively identified diffusional result, we are inclined to accept this mechanism in the present case.

Finally, we should point out that the above results and interpretation apply only to acetonitrile solvent and tetraethylammonium perchlorate or tetrafluoroborate electrolytes. The transport picture can be substantially altered by use of different solvents and electrolyte ions. For instance, acetonitrile swells the plasma polymerized vinylferrocene film; water solvent does not and the voltammetry in water is quite different (26).

We should be careful to note that the slow charge transport condition in Figure 8 may not simply be a result of the large film thickness indicated by the charge for ferrocene reaction. Thicker films are obtained with longer plasma deposition times, where plasma damage effects may accumulate. The slower charge transport may in part then be due to a larger separation between surviving ferrocene sites. We are presently attempting to determine equivalent weights for plasma polymer to probe this question.

ACKNOWLEDGEMENT. This research was supported in part by grants from the Office of Naval Research and National Science Foundation. R. J. N. acknowledges support of the National Research Countil in preparation of the manuscript; F. A. S. acknowledges sabbatical leave from Florida Atlantic University. This is Part XX of a series on Chemically Modified Electrodes. Presented in part at National ACS Meeting, Analytical Division, Honolulu, March, 1979.

REFERENCES

1 (a) L. L. Miller and M. R. Van De Mark, J. Electroanal. Chem., 88 (1978) 437; (b) Ibid., J. Amer. Chem. Soc., 100 (1978) 639; (c) M. R. Van De Mark and L. L. Miller, J. Amer. Chem. Soc., 100 (1978) 3223.

2 A. Merz and A. J. Bard, J. Amer. Chem. Soc., 100 (1978) 3222.

3 N. Oyama and F. C. Anson, J. Amer. Chem. Soc., 101 (1979) 739.

4 Symposium on Chemically Modified Electrodes, Extended Abstracts of Electrochemical Society National Meeting, Boston, Mass., May 1979.

5 F. B. Kaufman and E. M. Engler, J. Amer. Chem. Soc., 101 (1979) 547.

6 A. Diaz, private communication.

7 (a) M. S. Wrighton, R. G. Austin, A. B. Bocarsly, J. M. Bolts, O. Haas, K. D. Legg, L. Nadjo and M. C. Palazzotto, J. Electroanal. Chem., 87 (1978) 429; (b) Ibid., J. Amer. Chem. Soc., 100 (1978) 1602; (c) J. M. Bolts and M. S. Wrighton, J. Amer. Chem. Soc., 100 (1978) 5257; (d) J. M. Bolts, A. B. Bocarsly, M. C. Palazzotto, E. G. Walton, N. S. Lewis and M. S. Wrighton, J. Amer. Chem. Soc., 101 (1979) 1378.

8 K. Itaya and A. J. Bard, Anal. Chem., 50 (1978) 1487.

9 (a) R. Nowak, F. A. Schultz, M. Umana, H. Abruna and R. W. Murray, J. Electroanal. Chem., 94 (1978) 219; (b) R. W. Murray, Symposium on Silylated Surfaces, Midland Macromolecular Monograph, in press.

10 K. Doblhofer, D. Nölte and J. Ulstrup, Ber. Bunsenges. Phys. Chem., 82 (1978) 403.

11 A. B. Fischer, M. S. Wrighton, M. Umana and R. W. Murray, J. Amer. Chem. Soc., 101 (1979) 3442.

12 A. J. Bell and J. R. Hollahan, Eds., "Techniques and Applications of Plasma Chemistry", Wiley, New York, 1974.

13 H. Yasuda and T. Hirotsu, J. Polym. Sci., Polym. Chem. Ed., 16 (1978) 313, 743.

14 H. Hiratsuka, G. Akovali, M. Shen and A. T. Bell, J. App. Polym. Sci., 22 (1978) 917.

15 L. F. Thompson and K. G. Mayhan, J. App. Polym. Sci., 16 (1972) 2291.

16 W. S. Woodward, R. D. Rocklin and R. W. Murray, Chem., Biomed., and Environ. Instrumentation, 9 (1979) 95.

17 P. R. Moses, L. Wier and R. W. Murray, Anal. Chem., 47 (1975) 1882.

18 R. F. Lane and A. T. Hubbard, J. Phys. Chem., 77 (1973) 1401, 1411.

19 A. Bradley and J. P. Hammes, J. Electrochem. Soc., 110 (1963) 15.

20 J. R. Lenhard and R. W. Murray, J. Amer. Chem. Soc., 100 (1978) 7870.

21 M. Umana, D. Rolison, P. Daum, University of North Carolina, unpublished. results, 1978.

22 M. Umana, D. Rolison, R. Murray, Surface Science, submitted.

23 H. Yasuda and T. Hirotsu, J. Polym. Sci., Polym. Chem. Ed., 16 (1978) 229.

24 N. Oyama, A. P. Brown and F. C. Anson, J. Electroanal. Chem., 87 (1978) 435.

25 H. Yasuda and C. E. Lamaze, J. App. Polym. Sci., 15 (1971) 2277.

26 P. Delahay, "New Instrumental Methods in Electrochemistry", Interscience, 1954, page 119.

27 P. Daum, R. W. Murray, J. Electroanal. Chem., in press.

FIGURE LEGENDS

Figure 1. Geometries used in preparation of vinylferrocene polymer electrodes. XXXX indicates vinylferrocene monomer. Solid black regions are electrodes: A,B - glassy carbon; C - platinum.

Figure 2. Cyclic voltammetry for 15-second plasma deposition of vinylferrocene from Geometry B on glassy carbon electrode. 0.1 M Et_4NClO_4/CH_3CN, 0.05 volt/sec. $E^{\circ\prime}$ for ferrocene (average of peak potentials) = 0.424 ± 0.003 volt vs. SSCE for all sweep rates studied; coverage Γ = $0.5 \pm 0.04 \times 10^{-10}$ mole/cm.^{2} ; ΔE_p = 35 mv. Inset shows i_p vs. scan rate v .

Figure 3. SEM of glassy carbon electrode: before (A, upper right, inset) and after (A) plasma deposition of vinylferrocene polymer; B, after partial removal of film (see text). (10 minute reaction, Geometry B). Accelerating voltage = 20 KV; tilt angle 82° .

Figure 4. Cyclic voltammetry of plasma polymerized vinylferrocene dissolved in CH_2Cl_2 and reprecipitated by Merz-Bard (2) procedure, in 0.1 M Et_4NClO_4/CH_3CN . Apparent $\Gamma = 5 \times 10^{-9}$ mole/cm.^{2} at v = 0.2 volt/sec.

Figure 5. Cyclic voltammetry of plasma polymerized vinylferrocene deposited (3 minute reaction) from Geometry B on glassy carbon in 0.1 M Et_4NClO_4/CH_3CN containing 0.16 mM TCNQ at 0.2 volt/sec. Curve A: freshly deposited; Curve B: electrode of curve A after 3,000 potential cycles in absence of TCNQ.

Figure 6. Curves A, B: Dependence on axial distance for deposition (two minutes) on Pt from Geometry C. Curve A: 2 cm from monomer source, Γ = 30×10^{-10} mole/cm.^{2}, ΔE_p = 80 mv; Curve B: 8 cm, $\Gamma = 4.8 \times 10^{-10}$ mole/cm.^{2}, ΔE_p = 48 mv. Curves C, D: dependence on electrode material for deposition (3 minutes) from Geometry B. Curve C: Pt, $\Gamma = 6.8 \times 10^{-10}$ mole/cm.^{2}; Curve D: glassy carbon, $\Gamma = 4.7 \times 10^{-10}$ mole/cm.^{2}. All at 0.2 volt/sec. in 0.1 M Et_4NClO_4/CH_3CN.

Figure 7. Electrochemically measured coverage of plasma polymerized vinylferrocene as a function of plasma reaction time. Pt in 0.1 M Et_4NBF_4/CH_3CN; glassy carbon in 0.1 M Et_4NClO_4/CH_3CN . Numbers in parenthesis are XPES intensity ratios (corrected for cross-section) for Fe $2p_{3/2}$ / Pt 4F for indicated point. Open and solid circles represent platinum and glassy carbon electrodes, respectively.

Figure 8. Cyclic voltammogram of plasma polymerized vinylferrocene deposited (3 minute reaction) on Pt from Geometry C in 0.1 M Et_4NBF_4/CH_3CN . a-e: 0.320, 0.160, 0.080, 0.032 and 0.016 v/sec, respectively. Insets: upper left - dependence of electrochemical coverage on potential sweep rate; lower right - dependence of peak current on (potential sweep rate) 1/2 .

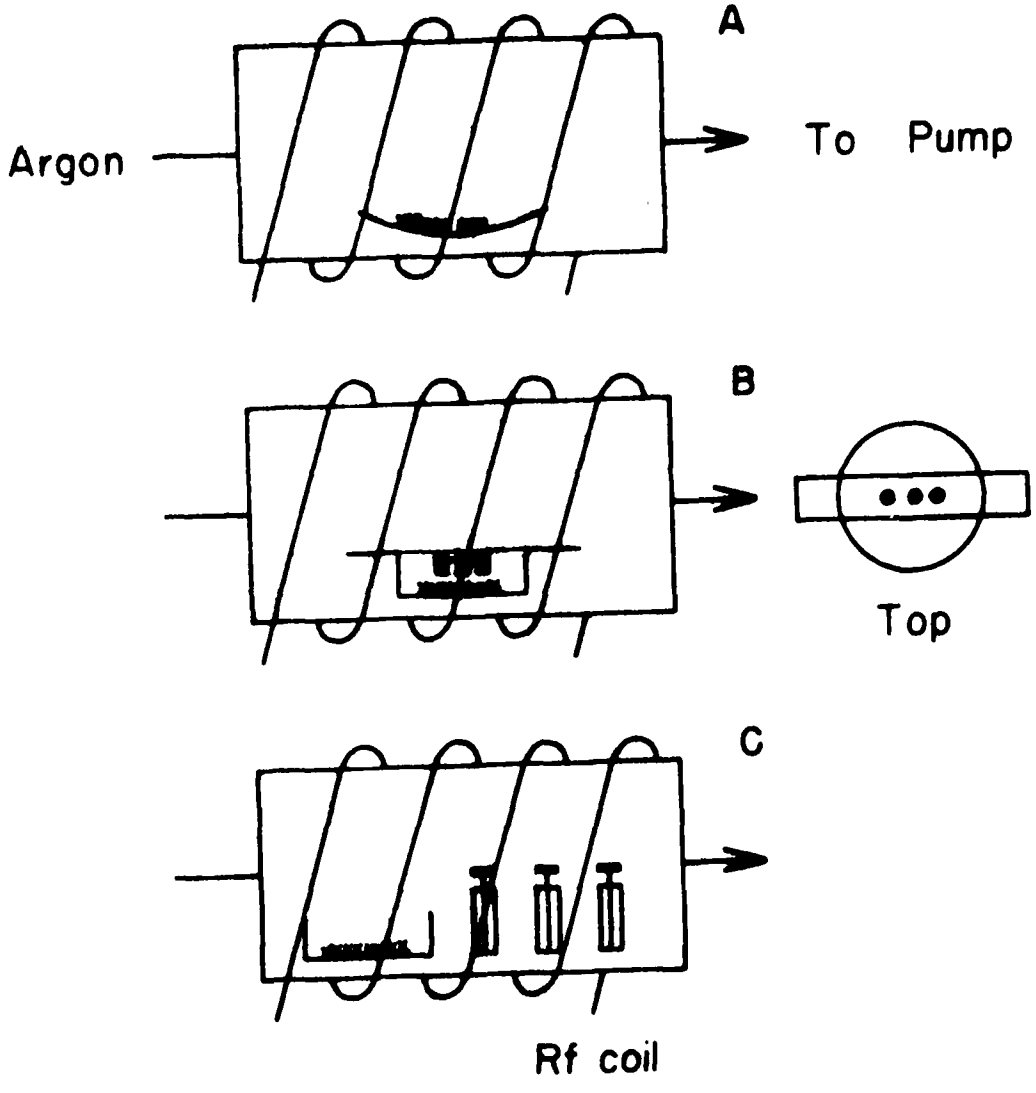
A
Argon
To Pump
B
Top
C
Rf coil

Fig

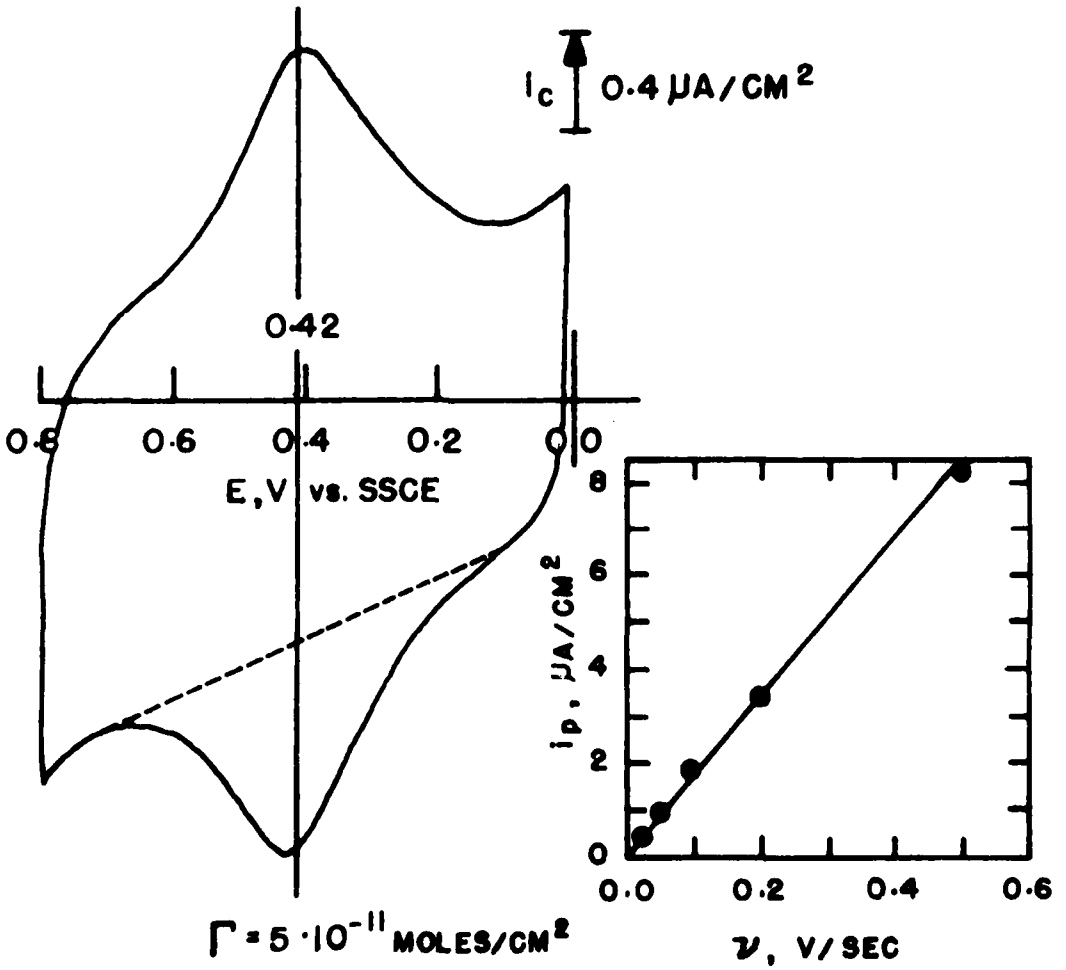
i_c 0.4 μA/CM²
0.42
0.8
0.6
0.4
0.2
0.0
E, V vs. SSCE
i_p, μA/CM²
8
6
4
2
0
0.0
0.2
0.4
0.6
ν, V/SEC
Γ = 5·10⁻¹¹ MOLES/CM²

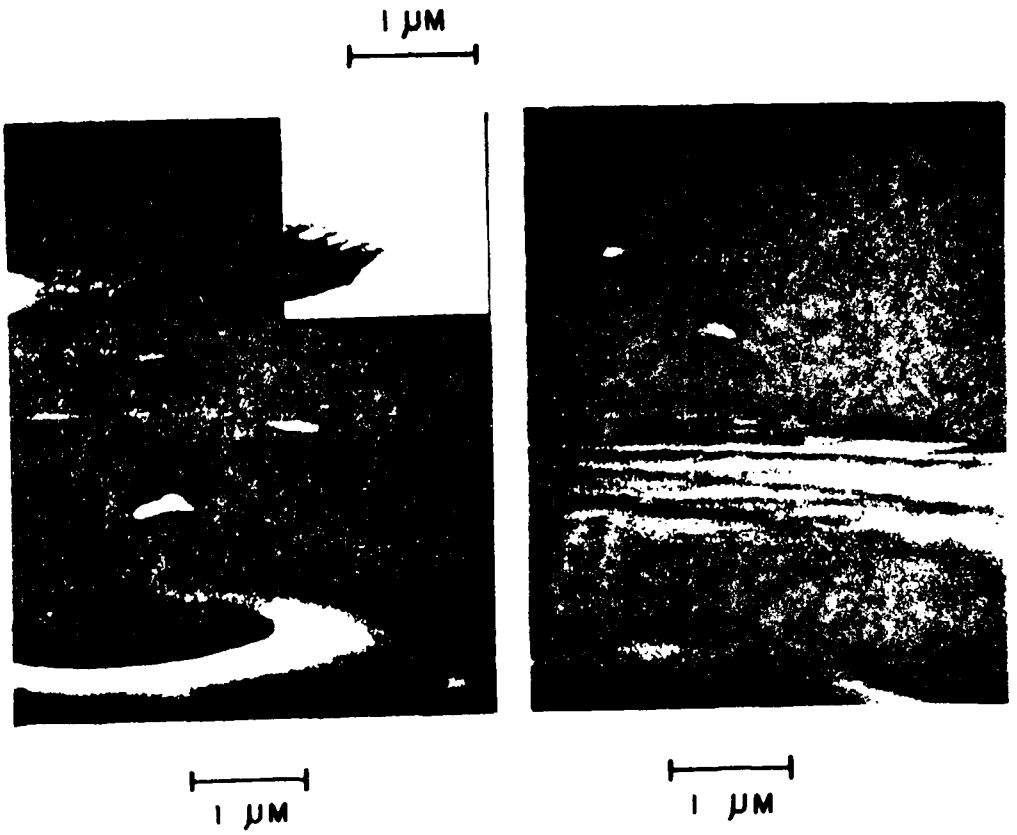

A B

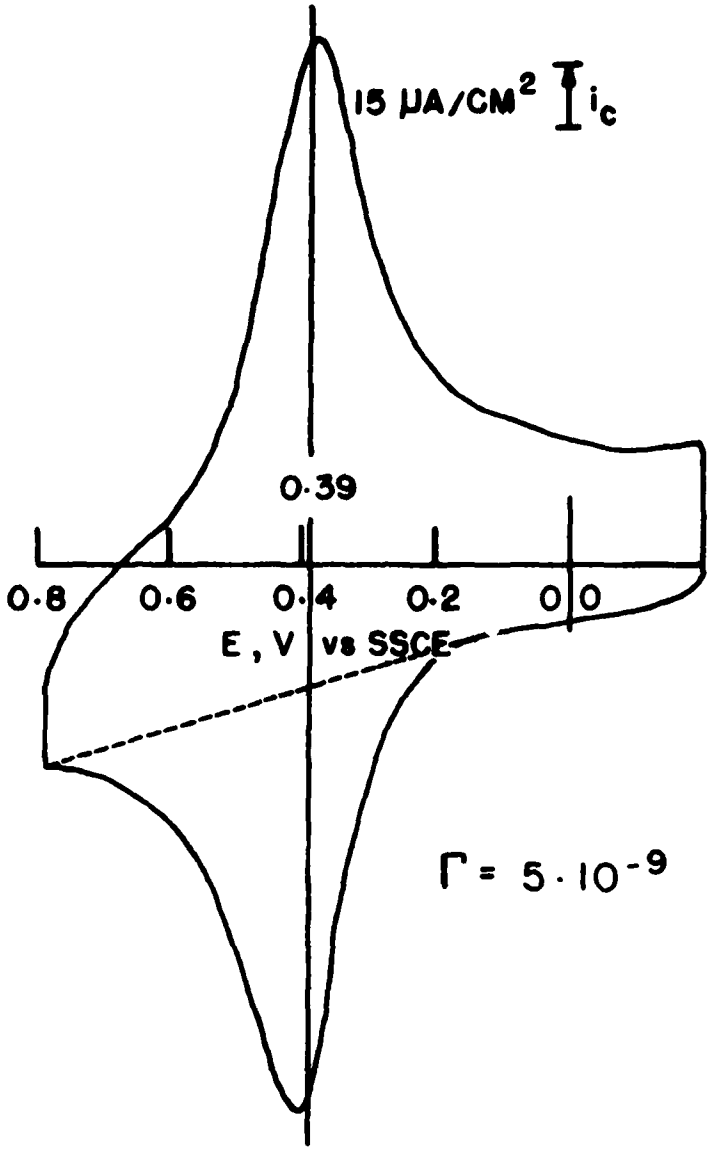

$\Gamma = 5 \cdot 10^{-9}$ MOLES/CM²

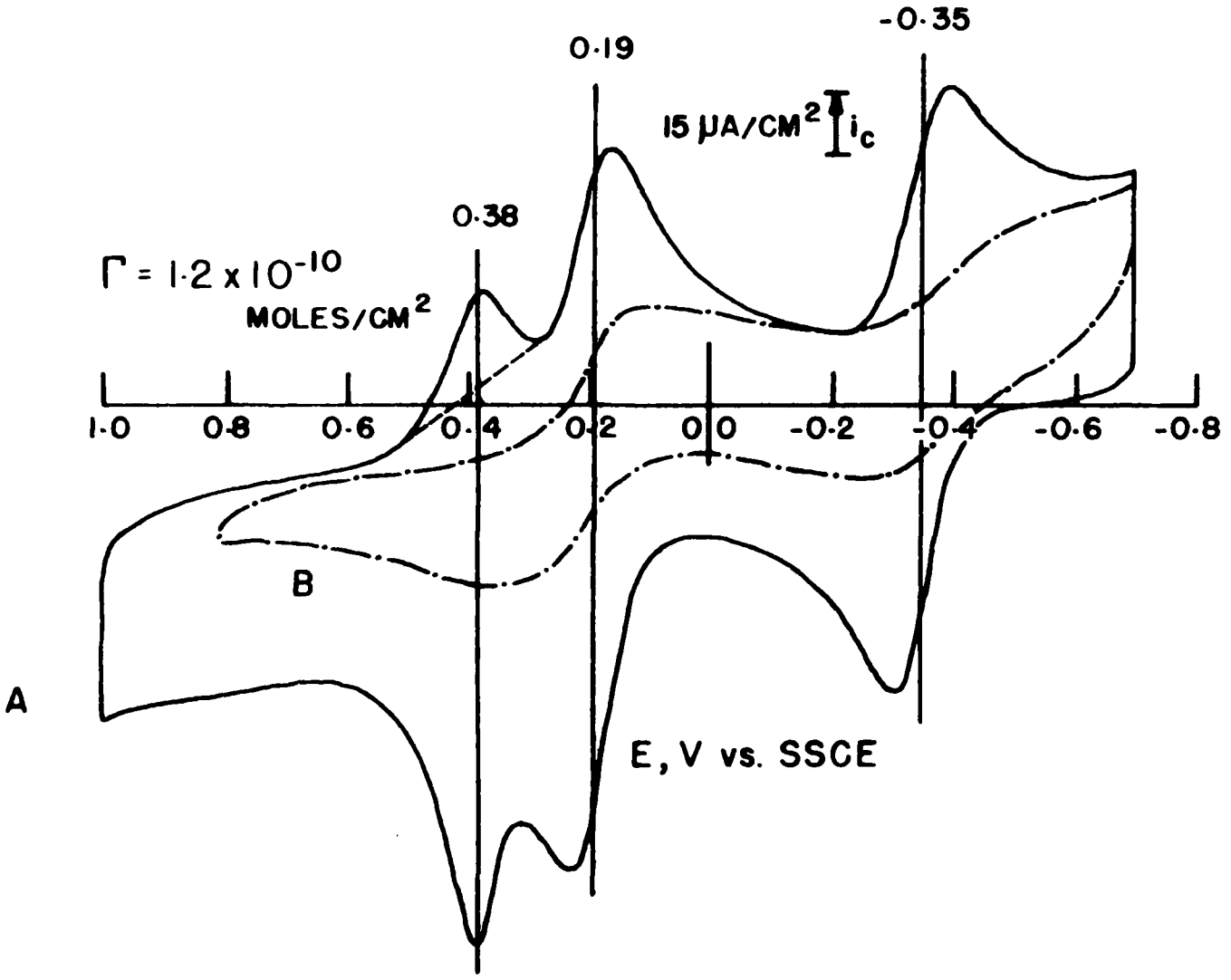
-0·35
0·19
15 μA/CM² i_c
0·38
Γ = 1·2 x 10⁻¹⁰
MOLES/CM²
1·0
0·8
0·6
0·4
0·2
0 0
-0·2
-0·4
-0·6
-0·8
B
A
E, V vs. SSCE

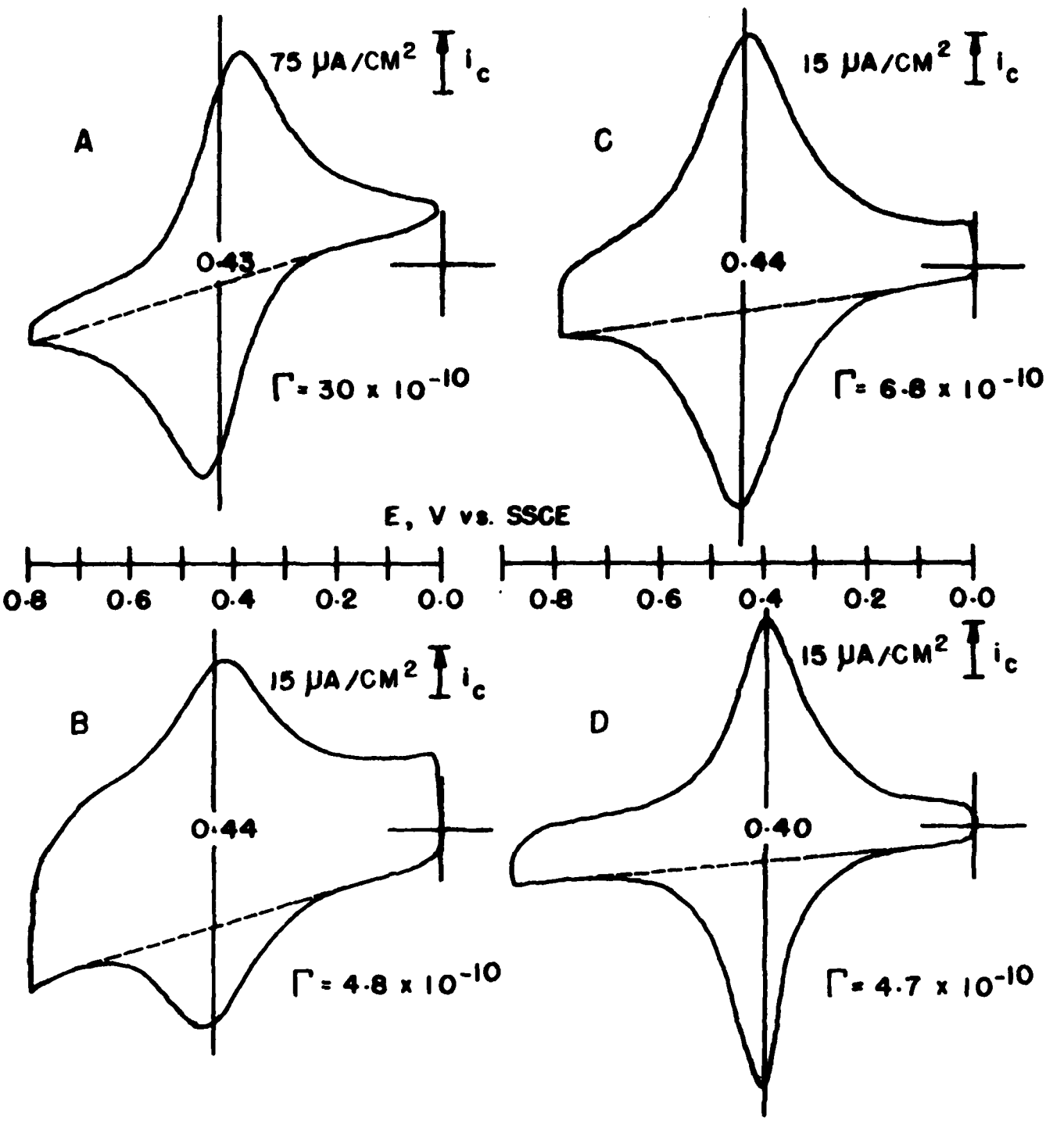
A
75 μA/CM² i_c
0.43
Γ = 30 x 10⁻¹⁰
C
15 μA/CM² i_c
0.44
Γ = 6.8 x 10⁻¹⁰
E, V vs. SSCE
0.8 0.6 0.4 0.2 0.0
0.8 0.6 0.4 0.2 0.0
B
15 μA/CM² i_c
0.44
Γ = 4.8 x 10⁻¹⁰
D
15 μA/CM² i_c
0.40
Γ = 4.7 x 10⁻¹⁰

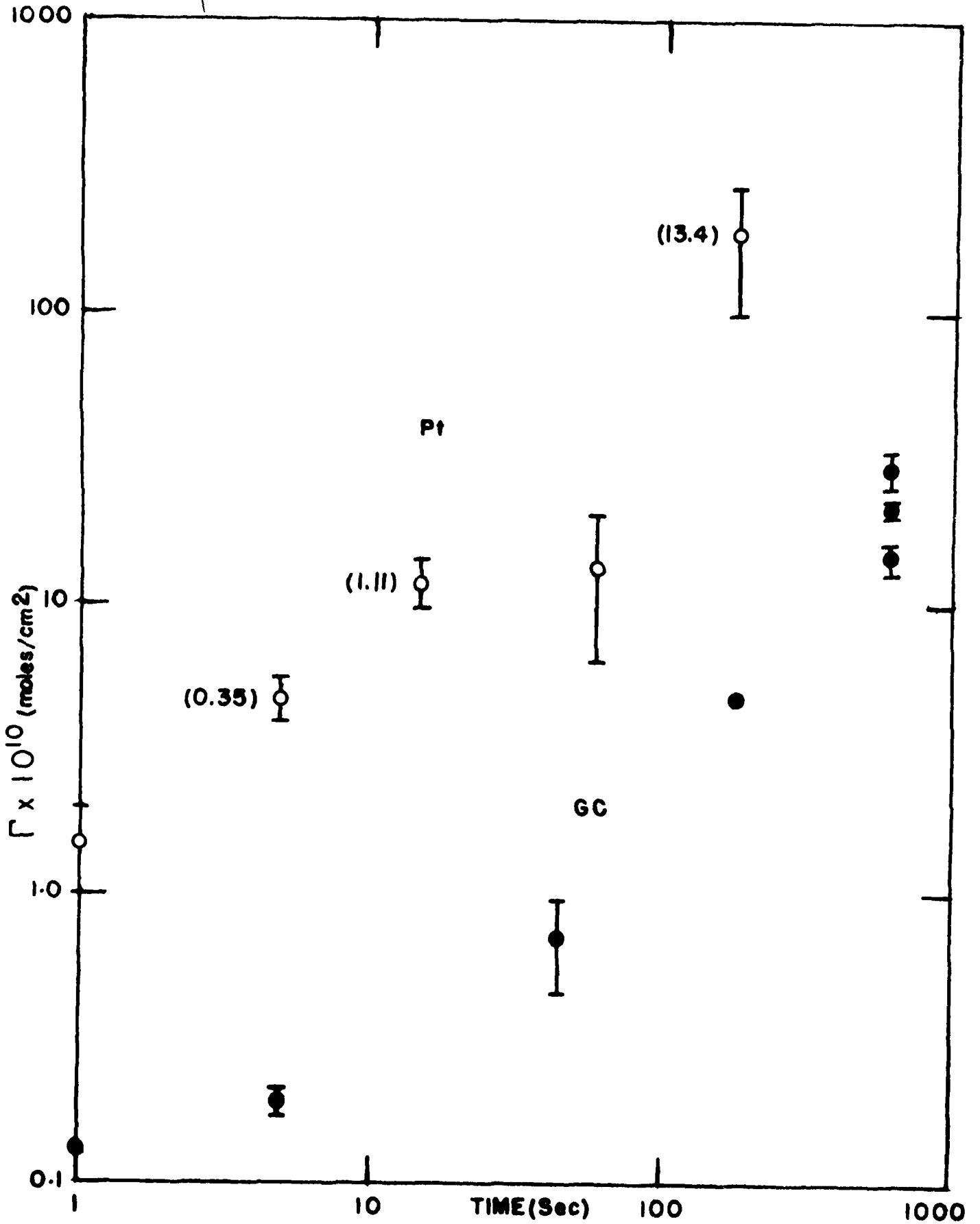
1000
100
10
1.0
0.1
Γ x 10^10 (moles/cm2)
(13.4)
(1.11)
(0.35)
Pt
GC
1
10
TIME(Sec)
100
1000

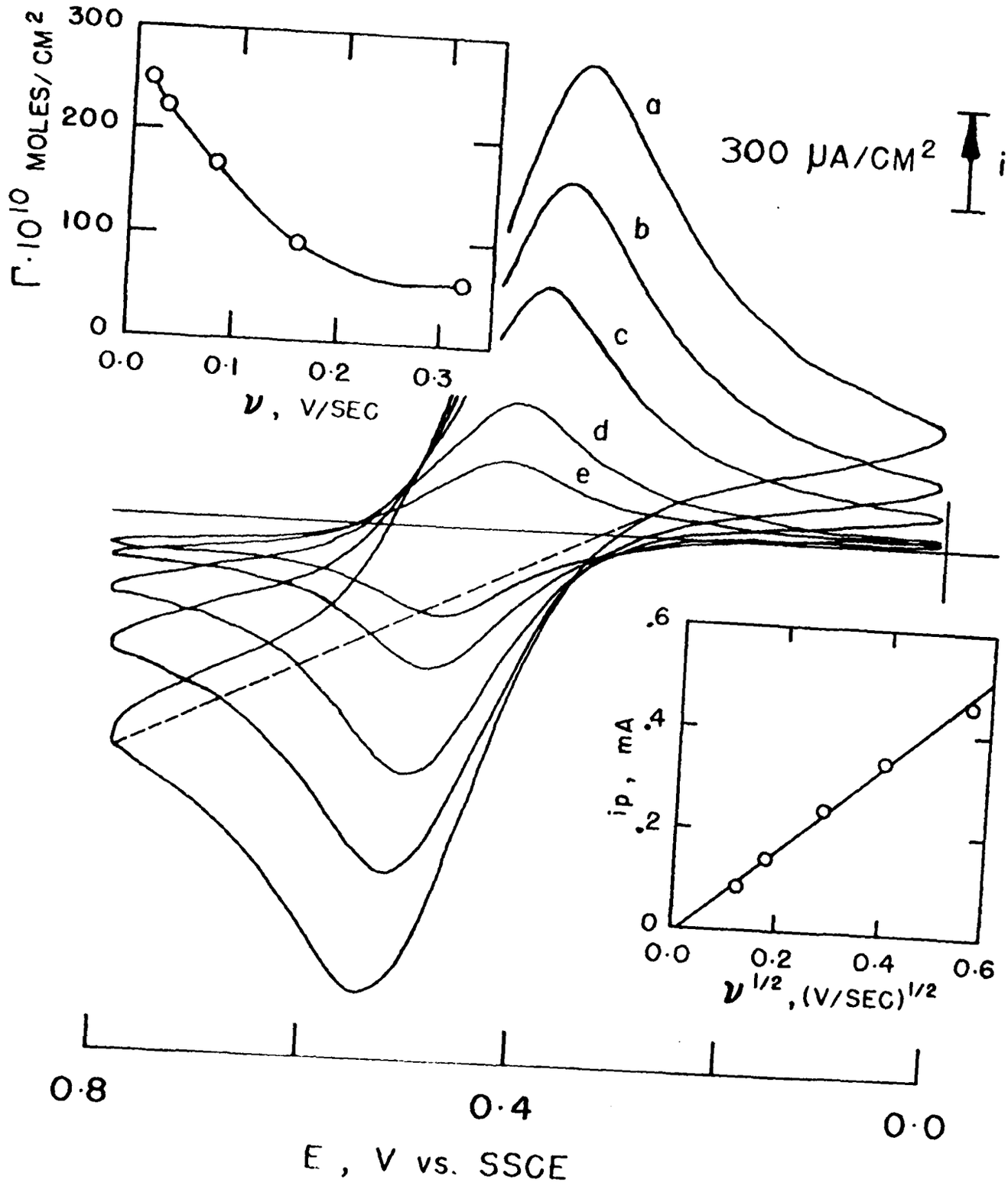
Γ·10^10 MOLES/CM^2
300
200
100
0
0.0
0.1
0.2
0.3
ν, V/SEC
a
b
c
d
e
300 μA/CM^2
i_c
.6
.4
.2
0
ip, mA
0.0
0.2
0.4
0.6
ν^1/2, (V/SEC)^1/2
0.8
0.4
0.0
E, V vs. SSCE